Inorganic Chemistry

ARTICLE

pubs.acs.org/IC

Conjugated Ligands Modulated Sandwich Structures and Luminescence Properties of Lanthanide Metal−Organic Frameworks

Tian-Fu Liu,[†] Wenjuan Zhang,[‡] Wen-Hua Sun,*[,‡] and Rong Cao*[,†]

[†]State Key Laboratory of Structural Chemistry, Fujian Institute of Research on the Structure of Matter, Chinese Academy of Sciences, Fujian, Fuzhou, 350002, P.R. China

[‡]Key Laboratory of Engineering Plastics and Beijing National Laboratory for Molecular Sciences, Institute of Chemistry, Chinese Academy of Sciences, Beijing 100080, P.R. China

Supporting Information

ABSTRACT:

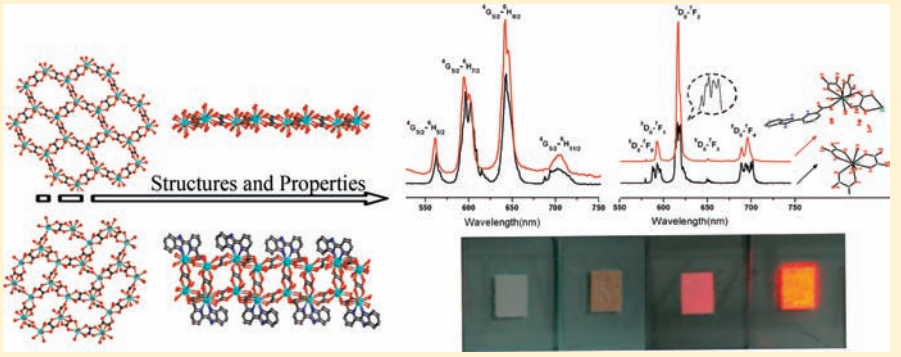

A conjugated ligand, 2-(carboxylic acid)-6-(2-benzimidazolyl) pyridine (Hcbmp), and a series of Lanthanide metal−organic frameworks (MOFs) $[Ln_2(cbmp)(ox)_3(H_2O)_2]_2 \cdot 2H_3O^+ \cdot 7H_2O$ (Ln = Sm (**3**), Eu (**4**), and Gd (**5**), H_2ox = oxalic acid) have been designed and assembled. To elucidate how the conjugated ligands modulate the structures and luminescence properties, we carried out the structural characterizations and luminescence studies of complexes **3** and **4**, and their corresponding oxalate complexes $[Ln(ox)_{1.5}(H_2O)_3] \cdot 2H_2O$ (Ln = Sm (**1**) and Eu (**2**)) were also investigated for comparison. The changes of luminescence behaviors upon dehydration and D_2O-rehydration processes are presented and discussed in detail. The results indicated that, the $cbmp^-$ ligands distribute on both sides of the ox^--Ln bilayer network to construct a sandwich structure. Moreover, the lowest triplet state of $cbmp^-$ ligands can match well the energy levels of the Sm^{3+} and Eu^{3+} cations which allow the preparation of new Ln-MOF materials with enhanced luminescence properties. Meanwhile, the crystallinity of solid states produces more substantial change in the luminescence behaviors than removal or replacement of effective nonradiative relaxers.

INTRODUCTION

Lanthanide complexes possess characteristic luminescence properties that make them crucial components for applications such as photonic materials, optical telecommunication devices, as well as biological imaging probes and sensors.[1] Since the emission mechanism of lanthanide ions is based on f-f transitions, lanthanide complexes give sharp emission lines without theoretical gap on the quantum efficiency. In addition, because lanthanides are inherently "hard" acids, diffuse interactions which often lead to line broadening are unfavorable in emission. Unfortunately, lanthanide electronic transitions are forbidden by parity (Laporte) selection rules, leading to weak absorbance and low quantum yields.[2] To circumvent this problem, the lanthanides need to be sensitized by a suitable chromophoric moiety (often referred as antenna). The sensitization involves placing lanthanide cations in proximity to chromophoric molecules having high absorptivity, and the antenna efficiently transfers energy to lanthanide accepting levels to trigger their emission.[3] The photophysical properties of lanthanide cations can be greatly affected by their coordination environment, the arrangement of chromophoric unit, vibration of −OH, −NH, and so on.[4] In this case, the metal−organic frameworks (MOFs) offer a unique platform and methodology for development of luminescent lanthanide materials as they have a degree of structural predictability and tunability.[5] In addition to the well-defined coordination environment of lanthanide ions, the structures of MOFs are readily tailored through variation of the linkers, templates, and growth conditions. Moreover, permanent porosity in MOFs allows luminescence properties to be modulated by guest species adsorbed in the pores.[6] Therefore, the MOFs not only possess the luminescent feature expected in traditional coordination chemistry but also

Received: March 22, 2011
Published: May 09, 2011

Table 1. Crystal Data and Structure Parameters for Complexes

	1	3	4	5
formula	$C_3H_{10}O_{11}Sm$	$C_{38}H_{44}N_6O_{41}Sm_4$	$C_{38}H_{44}N_6O_{41}Eu_4$	$C_{38}H_{44}N_6O_{41}Gd_4$
formula weight	372.47	1842.22	1848.62	1869.78
temperature (K)	298(2)	298(2)	298(2)	298(2)
wavelength (Å)	0.71073	0.71073	0.71073	0.71073
crystal system	orthorhombic	monoclinic	monoclinic	monoclinic
space group	$P2_1/c$	$C2/c$	$C2/c$	$C2/c$
a (Å)	11.093(3)	33.803(8)	33.805(6)	33.733(3)
b (Å)	9.6426(2)	8.8976(9)	8.8706(8)	8.8519(3)
c (Å)	10.1338(2)	19.658(5)	19.596(3)	19.5382(2)
α (deg)	90	90	90	90
β (deg)	90	115.975(9)	116.174(6)	116.318(3)
γ (deg)	90	90	90	90
volume (Å^3)	987.6(3)	5315.2(2)	5273.7(2)	5229.5(6)
Z	4	4	4	4
D_c (Mg/m^3)	2.437	2.267	2.293	2.339
μ (mm^{-1})	5.991	4.478	4.816	5.132
data collected	7569	17211	19246	19279
unique data (R_{int})	2254	4924	5993	5959
parameters	156	415	422	422
goodness-of-fit on F^2	1.027	1.113	1.109	1.130
R_1[a] $[I > 2\sigma(I)]$	0.0357	0.0409	0.0346	0.0362
wR_2[b]	0.0808	0.1074	0.1118	0.1393

[a] $R_1 = \Sigma||F_o| - |F_c||/\Sigma|F_o|$. [b] $wR_2 = \{\Sigma w(F_o^2 - F_c^2)^2/\Sigma w(F_o^2)^2\}^{1/2}$.

incorporate new properties that create the potential for quite different optical behaviors.

Some methods have been used to obtain intense luminescent Lanthanide MOFs (Ln-MOFs). For example, in mixed-lanthanide systems, instead of stimulating emission from each Ln(III) ion, energy can be transferred from one lanthanide to another, resulting in a preferential enhancement of a single lanthanide luminescence.[7] The enhancement is also observed within mixed lanthanide-transition-metal systems where lanthanide ion emission is sensitized via the ligand-to-metal charge transfer (LMCT) state.[8] Moreover, enhancement of luminescence can be accomplished through careful selection of organic ligands with conjugated motifs, such as aromatic carboxylic acids, β-diketones, and heterocyclic derivatives.[9] In this regard, the selection of the "antenna" ligands with suitable energy levels of their excited states plays a key role for the luminescence of materials.[10] Herein, a conjugated heterocyclic ligand, 2-(carboxylic acid)-6-(2-benzimidazolyl) pyridine (Hcbmp), and a series of Ln-MOFs $[Ln_2(cbmp)(ox)_3(H_2O)_2]_2 \cdot 2H_3O^+ \cdot 7H_2O$ (Ln = Sm (**3**), Eu (**4**), and Gd (**5**)) have been prepared and assembled. Although a number of Ln-MOFs have been documented, the investigations on the relationships between the crystal structures and the photoluminescence properties were relatively few.[11] For this purpose, the structural characterizations and luminescence studies of complexes **3** and **4** were carried out and their corresponding oxalate complexes $[Ln(ox)_{1.5}(H_2O)_3] \cdot 2H_2O$ (Ln = Sm (**1**) and Eu (**2**)) were investigated and compared. In view of the presence of coordinated and guest water molecules in **3** and **4**, luminescence properties of dehydrated and D_2O-rehydrated phases were also investigated to access the effects of crystallinity and guest molecules on the luminescence behaviors. The results indicated that the $cbmp^-$ ligands distribute on both sides of the ox^--Ln bilayer constructing a sandwich structure. The lowest triplet state of $cbmp^-$ ligands can match well the energy levels of Sm(III) and Eu(III) cations which allows the preparation of new Ln-MOF materials with enhanced luminescence properties. Meanwhile, the crystallinity of solid states produces more substantial change in the luminescence behaviors than removal or replacement of effective nonradiative relaxers. The studies presented herein may be useful for creating, optimizing, and tailoring the luminescent Ln-MOF materials.

EXPERIMENTAL SECTION

General Procedures. All chemicals were commercially purchased and used without further purification. Elemental analyses (C, N, and H) were carried out with an Elementar Vario EL III analyzer; IR spectra were recorded with PerkinElmer Spectrum One as KBr pellets in the range 400−4000 cm^{-1}. Single crystal X-ray diffractions were carried out by Rigaku Mercury CCD/AFC diffractometer. Thermogravimetric analysis (TGA) was carried out on a NETZSCH STA 449C instrument. The sample and reference (Al_2O_3) were enclosed in a platinum crucible and heated at a rate of 10 °C/min from 30 °C temperature to 1000 °C under nitrogen atmosphere.

Luminescence emission and excitation spectra and transient decays were recorded on an Edinburgh Instruments spectrofluorimeter FLS920 equipped with both continuous (450 W) and pulsed xenon lamps. The absolute quantum yield (QY) of $ZrO_2:Eu^{3+}$ NPs was measured at room temperature by employing a barium sulfate coated integrating sphere (Edinburgh) as the sample chamber that was mounted on the fluorimeter (FLS920) with the entry and output port of the sphere located at a 90° geometry from each other in the plane of the spectrometer. For low temperature measurements, samples were mounted on a closed cycle cryostat (10−350 K, DE202, Advanced Research Systems).

dx.doi.org/10.1021/ic200579j |Inorg. Chem. 2011, 50, 5242–5248

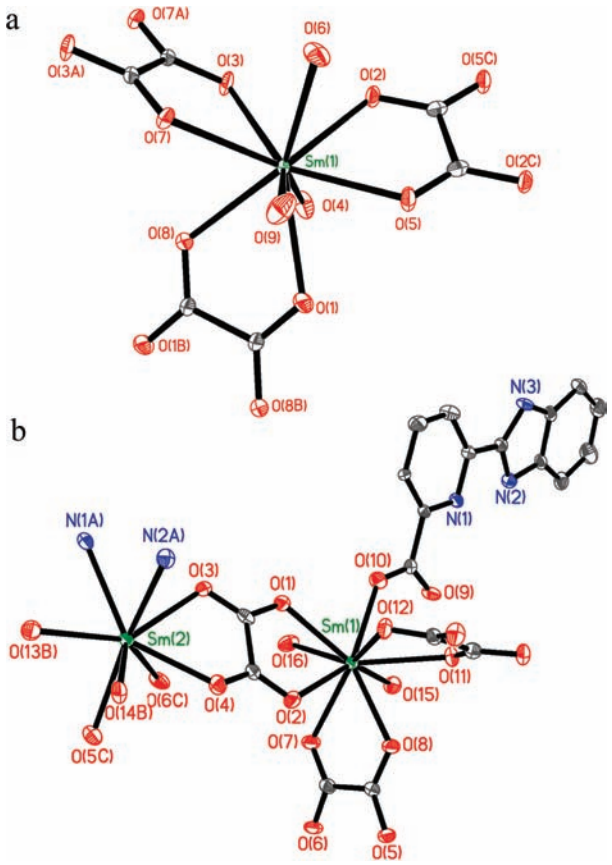

Figure 1. Representation of the Eu(III) coordination environments and ligands' coordination modes of **1** (a) and **3** (b). A = $-x, -y, 1-z$, B = $-x, -y, 2-z$, C = $1-x, -y, 2-z$ for **1**; A = $x, -y, 1/2+z$, B = $x, -y-1, 1/2+z$, C = $-x, y, 1/2-z$ for **3**.

Synthesis of Hcbmp. The ligand was prepared using the same procedure recorded in our early report.[12]

Synthesis of $[Sm(ox)_{1.5}(H_2O)_3]\cdot 2H_2O$ (1). A mixture of $Sm(NO_3)_3\cdot 6H_2O$ (0.4 mmol), H_2ox (0.6 mmol), 1 mL of NaOH solution (1 mmol·L^{-1}), and 10 mL of deionized water (pH ≈ 4.5 for the mixture) was sealed in a 25 mL Teflon-lined stainless steel autoclave and heated at 155 °C for 2 days. After cooling to room temperature, colorless crystals of **1** were obtained in 83.4% yield based on H_2ox. Elemental analysis for $C_3H_{10}O_{11}Sm$: Calcd: C, 9.67%; H, 3.72%, Found: C, 9.97%; H, 4.11%.

Synthesis of $[Eu(ox)_{1.5}(H_2O)_3]\cdot 2H_2O$ (2). The compound was prepared in the same way as that for **1** by using $Eu(NO_3)_3\cdot 6H_2O$ (0.4 mmol) as metal source. Colorless crystals of **2** were obtained in 82.5% yield based on oxalic acid. Elemental analysis for $C_3H_{10}O_{11}Eu$: Calcd: C, 9.62%; H, 3.74%, Found: C, 10.11%; H, 3.87%.

Synthesis of $[Sm_2(cbmp)(ox)_3(H_2O)_2]_2\cdot 2H_3O^+\cdot 7H_2O$ (3). A mixture of $Sm(NO_3)_3\cdot 6H_2O$ (0.4 mmol), H_2ox (1.6 mmol), and Hcbmp (0.2 mmol) in deionized water (10 mL) was adjusted to pH = 6.0 with 1 mmol·L^{-1} NaOH solution. It was then sealed in a 25 mL Teflon-lined stainless steel autoclave and heated at 175 °C for 3 days. After cooling to room temperature, colorless crystals of **3** were obtained in 59.3% yield based on Hcbmp Elemental analysis for $C_{38}H_{44}N_6O_{41}Sm_4$: Calcd: C, 24.75%; H, 2.39%; N, 4.56%, Found: C, 24.21%; H, 2.21%; N, 4.16%. IR (KBr, cm^{-1}): 3062(w), 1611(s), 1316(s), 793(m).

Synthesis of $[Eu_2(cbmp)(ox)_3(H_2O)_2]_2\cdot 2H_3O^+\cdot 7H_2O$ (4). The compound was prepared in the same way as that for **3** by using $Eu(NO_3)_3\cdot 6H_2O$ (0.4 mmol) as metal source. Colorless crystals of **4** were obtained in 60.7% yield based on Hcbmp. Elemental analysis for $C_{38}H_{44}N_6O_{41}Eu_4$: Calcd: C, 24.67%; H, 2.38%; N, 4.54%, Found: C, 23.98%; H, 2.04%; N, 4.31%. IR (KBr, cm^{-1}): 3066(w), 1612(s), 1318(s), 795(m).

Synthesis of $[Gd_2(cbmp)(ox)_3(H_2O)_2]_2\cdot 2H_3O^+\cdot 7H_2O$ (5). The compound was prepared in the same way as that for **3** by using $Gd(NO_3)_3\cdot 6(H_2O)$ (0.4 mmol) as metal source. Colorless crystals of **5** were obtained in 61.2% yield based on Hcbmp. Elemental analysis for $C_{38}H_{44}N_6O_{41}Gd_4$: Calcd: C, 24.39%; H, 2.35%; N, 4.49%, Found: C, 23.94%; H, 2.18%; N, 4.27%. IR (KBr, cm^{-1}): 3102(w), 1615(s), 1318(s), 196(m).

X-RAY CRYSTALLOGRAPHIC STUDIES

Data for complexes **1**, **3**, **4**, and **5** were collected on a Rigaku Mercury CCD diffractometer equipped with graphite-monochromated Mo Kα radiation with wavelength of 0.71073 Å by using the ω-scan technique. All absorption corrections were performed using the CrystalClear program.[13] Structures were solved by direct methods and refined on F^2 by full matrix least-squares using the SHELXL-97 program package.[14] The organic hydrogen atoms were positioned geometrically. Details of the structure solution and final refinements for the complexes are given in Table 1. Complex **1** has been reported by Weigel et al.[15] The CCDC 793865−793867 contain the crystallographic data **3**−**5** for this paper. These data can be obtained from the Cambridge Crystallographic Date Center via www.ccdc.cam.ac.uk

RESULTS AND DISCUSSION

Single crystal X-ray diffraction analysis reveals that complex **1** crystallizes in monoclinic space group $P2_1/c$. The asymmetric unit of **1** consists of a Sm(III) atom, three halves of ox^- ligands, three coordinated water molecules, and two lattice water molecules. The Sm(III) center is nine-coordinated to give a tricapped triprismatic geometry (Figure 1a). Six ox^- ligands bridge six metal centers forming a six-membered ring with the Sm−Sm distances of 6.346 Å and 6.488 Å. The fused six-membered rings prolongate along the [001] direction generating a two-dimensional (2D) honeycomb monolayer (Figure 2). The structure is stabilized by H-bonds between coordinated and lattice water molecules. Complex **2** is isostructural with **1** as evidenced by powder X-ray diffraction (in Supporting Information, Figure S1).

Complexes **3**, **4**, and **5** are isostructural (Supporting Information, Figure S2). As a representative example, the crystal structure of **3** is depicted in detail. The asymmetric unit consists of two crystallographically independent Sm(III), a $cbmp^-$ ligand, three ox^- ligands, six and a half water molecules, and a proton (results of bond valence calculations indicate that Sm1 and Sm2 are in a stable oxidation state of +3 with the total bond valences of 3.17 and 3.33, respectively.[16] The capture of a proton, which is usually encountered in other MOFs,[17] is the only way to balance the overall charges of complex **3**). The Sm(III) centers are all nine-coordinated in a tricapped triprismatic geometries. The Sm1 is bonded by six oxygen atoms from three ox^- ligands, two water molecules, and a carboxylate oxygen atom from a $cbmp^-$ ligand. The Sm2 is bonded by six oxygen atoms from three ox^- ligands, a carboxylate oxygen atom, and two nitrogen atoms from a $cbmp^-$ ligand (Figure 1b). Two carboxylate groups from two $cbmp^-$ ligands and four ox^- ligands form a six-membered ring. The Sm−Sm distances are 6.223 Å and 6.229 Å which are slightly shorter than those of **1**. The fused rings, slightly distorted, construct a lamellar layer, and the adjacent layers are connected by ox^- ligands resulting in the formation of an ox^--Sm bilayer.

dx.doi.org/10.1021/ic200579j |Inorg. Chem. 2011, 50, 5242–5248

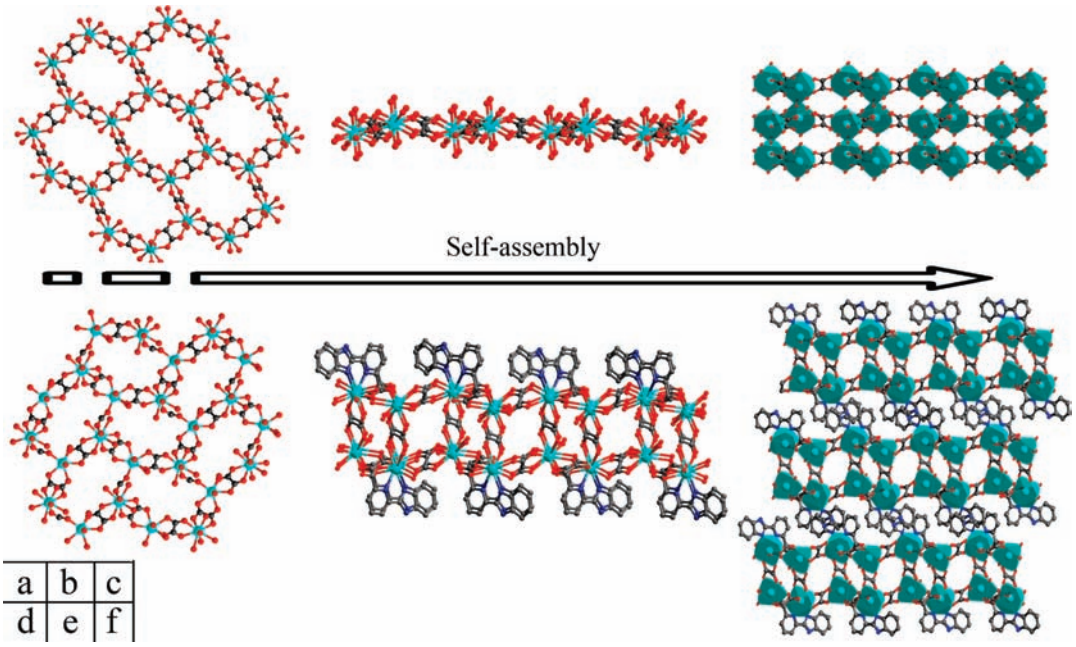

Figure 2. Top: representation of the fused six-membered rings (a), the 2D monolayer (b), and the crystal packing in polyhedral mode (c) of **1**. Bottom: representation of the fused six-membered rings (d), the 2D sandwich bilayer (e), and the crystal packing in polyhedral mode (f) of **3**.

The $cbmp^-$ ligands chelate on both sides of the bilayer to construct a 2D sandwich type structure. The neighboring layers are interlaced with the conjugated backbones of $cbmp^-$ ligands. As a result, beside H-bonds, $\pi-\pi$ interactions simultaneously widely exist between the interlayers to support the overall structure (Figure 2).

It is interesting to note that complexes **1** and **3** have some commonalities in their structures. The mole ratios of Sm(III) and ox^- are both 1:1.5, although the loading compounds were different in the two reaction systems. They are both 2D layered structures based on six-membered rings with similar Sm−Sm separations (6.229−6.488 Å). Differently, in **1**, the six-membered rings are composed by six ox^- ligands, while in **3** two ox^- ligands are replaced by two carboxylate groups from $cbmp^-$ ligands. The remaining ox^- ligands are employed to connect neighboring layers to construct the bilayer network, so the Sm(III):ox^- ratio of **3** is identical with that of **1**. It is supposed that some specific tendencies are retained in the self-assembly processes of **1** and **3**. The introduction of conjugated ligands can modulate the MOFs structure without changing the structural dimensionality, the building blocks, and the distance of metal centers.

Luminescence Properties. Intramolecular energy transfers from the triplet state of ligands to the resonance level of Ln(III) ions have great influence on Ln(III) luminescence according to Dexter and Sato's results.[9b,18] Herein, the low temperature (78 K) luminescence spectrum of Hcbmp was measured to investigate the energy difference (Supporting Information, Figure S4). From the estimation of the maximum emission bands (441 nm for Hcbmp), the lowest triplet state of energy can be determined as 22676 cm^{-1} for Hcbmp.[19] The lowest triplet state for H_2ox is 24570 cm^{-1} as documented in literature.[20] As we know, the intramolecular energy transfer efficiency depends mainly on two processes. One is the energy transition from the lowest triplet state energy of the ligand to the resonant energy level of the Ln(III) ion. The other is the inverse energy transition from the Ln(III) ion to the ligand by the thermal deactivation mechanism.

Table 2. Energy Difference between the Lowest Triplet Energy of H_2ox/Hcbmp Ligands and the Resonant Energy Level of the Ln (III) Ion

complex	lowest triplet state energy (cm^{-1})	resonant level (cm^{-1})	ΔE (Tr-Ln^{3+})
Ox-Sm (**1**)	24570	17850	6720
Ox-Eu (**2**)	24570	19020	5550
Ox-Gd	24570	32066	
cbmp-Sm(**3**)	22676	17850	4826
cbmp-Eu (**4**)	22676	19020	3656
cbmp-Gd	22676	32066	

If the energy difference is too small, the inverse energy transfer will take place much easier.[9,21] The energy difference minimizing the back transfer process is around 2500−3500 cm^{-1}. Therefore there exists optimal energy difference between the triplet position of ligands and the emissive energy level of Ln^{3+} ions (ΔE(Tr-Ln^{3+})). As shown in Table 2, the energy differences ΔE(Tr-Ln^{3+}) of ox^- complexes are much larger than those of the $cbmp^-$ complexes. It can be predicted that the lowest triplet energy level of $cbmp^-$ ligands can match well to the resonance levels of Sm(III) and Eu(III), so the $cbmp^-$ complexes exhibit better luminescence properties than their corresponding ox^- complexes. As the resonance level of Gd(III) (32066 cm^{-1}) is much higher than the triplet states of the H_2ox and Hcbmp ligands, the energy transfer from the triplet state of H_2ox or Hcbmp to the Gd(III) ion is energetically impossible. Therefore, the luminescence property of Gd(III) complex will not be discussed herein.

The measurement of the excitation spectrum allows accurate determination of the maximum of excitation for **1**−**4**. When **1** and **3** were excited at 403 and 365 nm, respectively, their solid-state emission spectra exhibited typical emission patterns characteristic of the Sm(III) ions with narrow, sharp, and well-separated bands (Figure 3a). The emissions that appeared in the

dx.doi.org/10.1021/ic200579j |*Inorg. Chem.* 2011, 50, 5242–5248

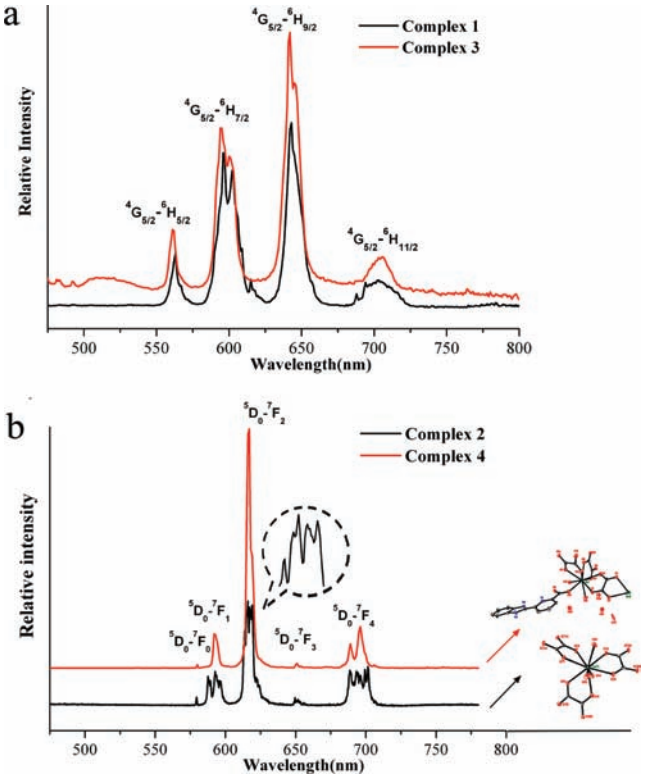

Figure 3. Emission spectra of **1**, **3** (a) and **2**, **4** (b). Emission slit width: 0.5 mm (for **1** and **3**), 0.07 mm (for **2** and **4**). Increment: 1 nm (for **1** and **3**) and 0.5 (for **2** and **4**). Temperature: 298 K.

range of 550−720 nm can be ascribed to the $^4G_{5/2}$−$^6H_{5/2,\,7/2,\,9/2,\,11/2}$ transitions. Figure 3b shows the emission spectra for **2** and **4** excited at 395 and 365 nm, respectively. Transitions from the excited $^5D_0$ state to the different J (0−4) levels of the lower ^7F_J state were observed in the range of 570−700 nm. The emission intensity of the so-called hypersensitive $^5D_0$−$^7F_2$ transition is much stronger than that of the $^5D_0$−$^7F_1$ transition, indicating that Eu(III) ions locate at low-symmetry sites without inversion center. The $^5D_0$−$^7F_0$ transition of Eu(III) induced by crystal field J mixing is present in the emission spectrum, which is only allowed for the 10 symmetries, C_s, C_1, C_2, C_3, C_4, C_6, C_{2v}, C_{3v}, C_{4v}, and C_{6v}, according to the ED selection rule.[22] Actually, the crystallographic studies reveal that both **2** and **4** belong to the C_s symmetry with Eu(III) ions occupying low-symmetry sites. However, the emission spectrum of **2** is different from that of **4** in terms of splitting numbers of peaks, and it is interesting to observe that the emission spectra could provide information about the structural difference of their coordination sites. Three lines splitting for the $^5D_0$−$^7F_1$ transition suggest the formation of a well-defined and rigid species with low symmetry. The five lines splitting for the $^5D_0$−$^7F_2$ transition indicate that there is only one type of coordination environment for Eu(III) cations in complex **2** with C_s, C_1, or C_2 symmetry.[23] In contrast, the absence of splitting emission bands for the $^5D_0$−$^7F_1$ and $^5D_0$−$^7F_2$ transitions in the spectrum indicates that there are at least two different types of Eu(III) species in **4**. In fact, these results are in good agreement with the single-crystal X-ray analyses in which the asymmetric unit of **2** contains only one Eu(III) center, while the asymmetric unit of **4** contains two Eu(III) centers with different coordination environments.

The emission quantum yields (Φ_{QY}) were measured at room temperature under the excitation wavelengths that maximize the

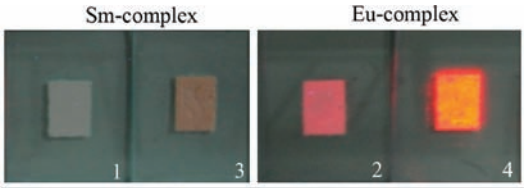

	Φ_{QY} (%)	λ_{ex} (nm)	τ_1 (ms)	τ_2 (ms)
1	—	403	0.004	
3	0.43	365	0.007 (56.39%)	0.16 (43.61%)
2	6.08	395	0.27	
4	29.72	365	0.20 (3.61%)	0.56 (96.39%)

Figure 4. Images of complexes **1**−**4** under UV lamp at 365 nm and the table of their quantum yields and lifetimes.

emissions of lanthanide cations. The quantum yield of **1** is lower than the detection limit of our equipment, which may be attributed to the very large energy difference between the triplet energy level of the ox$^-$ ligands and the resonance level of Sm(III) ions ΔE(Tr-Ln^{3+}) (6720 cm^{-1}). However, in complex **3**, the energy difference ΔE(Tr-Ln^{3+}) is much smaller than that of **1** because of the introduction of conjugated cbmp$^-$ ligands. As a result, the Φ_{QY} has a value of 0.43% for complex **3**. Similarly, the quantum yield of **4** (29.72%) is much higher than that of **2** (6.08%) because of the lower energy difference ΔE(Tr-Ln^{3+}) caused by the introduction of cbmp$^-$ ligands. To better understand the luminescence properties of **1**−**4**, the lifetime values were determined from the luminescence decay profiles (see Supporting Information) at room temperature. The decay patterns displaying monoexponential behavior for **1** and **2** indicate the presence of a single chemical environment around the Ln(III) ions, while the biexponential decay patterns for **3** and **4** indicate the presence of two kinds of chemical environments around the Ln(III) ions.[4a,24] Those results fit well with the X-ray structure analyses. Moreover, as listed in Figure 4, the lifetimes of complexes **3** and **4** are longer than their corresponding ox$^-$ complexes **1** and **2**. The structural feature may account for the difference in lifetime: (a) π−π interactions of the conjugated ligands bring lumophores closer, enabling electronic interactions between the lumophores, which result in the increase of emission lifetime.[2,9] (b) The rigid cbmp$^-$ ligands chelate to Ln(III) centers and lead to the replacement of some coordinated water molecules as compared with ox$^-$ complexes (**1** and **2**). Reducing the number of OH oscillators in the first coordination sphere of the metal ion virtually decreases the nonradiative decay rate and increases the lifetime of the sample.[25] Those results demonstrated that the conjugated cbmp$^-$ ligand, which improved greatly the quantum yields and lifetimes of Sm(III) and Eu(III) complexes, is an efficient sensitizer in luminescent Ln-MOFs.

Luminescence properties of MOFs can also be dramatically affected by the coordination environment of the metal centers, arrangement of lumophores, species of guest molecules, and so forth. In general, water molecules are very effective nonradiative relaxers to quench luminescence because of the loss of excited-state energy from the Ln(III) ions through vibrational energy of the close proximity OH oscillator, while the D_2O molecules are generally less effective nonradiative relaxers.[25] To further understand the effects of the water molecules on the luminescence properties, we investigated the quantum yields and lifetimes of **3** and **4**, upon the dehydrated and D_2O-rehydrated processes. Thermogravimetric analysis (TGA) studies for **3** and **4** indicate

dx.doi.org/10.1021/ic200579j |*Inorg. Chem.* 2011, 50, 5242–5248

Table 3. Quantum Yields and Lifetimes of the As-Synthesized, Dehydrated and D_2O-Rehydrated Phases of Complexes 3 and 4

	complex	Φ_{QY} (%)	τ_1 (ms)	τ_2 (ms)
3	as-synthesized	0.43	0.007 (56.39%)	0.016 (43.61%)
	dehydrated	0.09	0.018 (48.93%)	0.005 (51.07%)
	D_2O-rehydrated	0.22	0.012 (96.04%)	0.067 (3.96%)
4	as-synthesized	29.72	0.20 (3.61%)	0.56 (96.39%)
	dehydrated	0.15	0.22 (8.22%)	0.56 (91.78%)
	D_2O-rehydrated	7.63	0.53 (97.70%)	0.12 (2.30%)

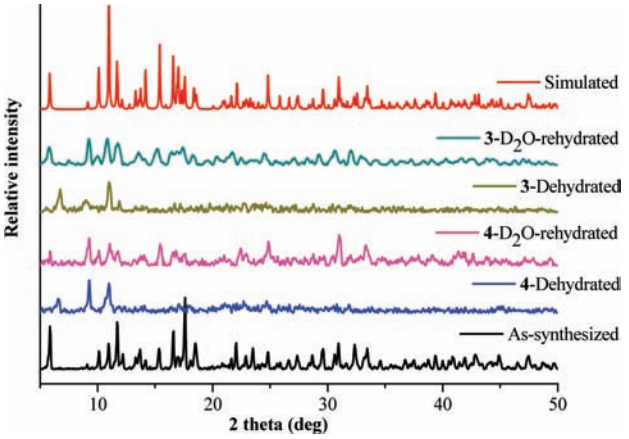

Figure 5. XRPD patterns for the as-synthesized, the dehydrated and D_2O-rehydrated phases for complexes **3** and **4**, and the simulated patterns from single-crystal X-ray data.

that the first weight loss of about 8.2% before 150 °C corresponds to the removal of the guest water molecules (calc: 8.8%), and the continuous weight loss of 3.6% (calc: 3.9%) in the temperature range of 150−190 °C corresponds to the removal of the coordinated water molecules, which are in agreement with the two endothermic peaks observed at 142 and 185 °C in the differential thermal analysis (DTA) diagrams (Supporting Information, Figure S3). When the samples were evacuated at 185 °C to remove the guest and coordinated water molecules, the quantum yields decreased dramatically. When the samples were subsequently rehydrated with D_2O, the quantum yields were recovered but still were lower than those of the as-synthesized samples. However, no noticeable changes in lifetime were observed during the processes as illustrated in Table 3 (see the luminescence decay profiles in Supporting Information, Figures S9 and S10). Removal and replacement of H_2O molecules did not reduce the nonradiative decay rates, as is usually believed, but greatly changed the quantum yields. The interesting phenomena may be related to the D_2O-induced structural phase transformation. As illustrated in Figure 5, complexes **3** and **4** transformed to other (nearly amorphous) phases when the guest and coordination water molecules were removed. Remarkably, they can easily recover the crystalline state by immersion in D_2O. However, the lower intensity in the XRPD patterns indicated that the crystallinity is not as good as that of original phase, and there are some amorphous components in the rehydrated samples. Typically, the amorphous and poor crystallinity will result in the loss of $\pi-\pi$ interactions between neighboring chromophores and the existence of a large number of hanging bonds. Those factors dramatically decrease the ligands-to-metal energy transfer efficiency.[1a,26] Therefore, it is reasonable to presume that the crystallinity in the solid state produces more substantial change in the luminescence behaviors than removal or replacement of effective nonradiative relaxers.

CONCLUSION

Organic sensitizer with a conjugated backbone, such as aromatic carboxylic acid and the heterocyclic derivative, usually plays a critical role in Ln-MOFs luminescence. Herein the π-rich ligands Hcbmp and the bridging ligands H_2ox, were employed to synthesize new lanthanide complexes. To elucidate the effects of the conjugation ligands on the structures and luminescence properties, the structural characterizations and luminescence studies of Sm(III) and Eu(III) complexes (**3** and **4**) were carried out, and their corresponding oxalate complexes (**1** and **2**) were investigated for comparison. Single-crystal X-ray analyses reveal that **1** is composed by fused six-membered rings forming a 2D honeycomb layer. Complex **3** consists of a bilayer network with $cbmp^-$ ligands chelating on the two sides forming a sandwich structure. Luminescence investigations demonstrate that the conjugated $cbmp^-$ ligand exhibits a good antenna effect with respect to the Sm(III) and Eu(III) cations because of the suitable energy difference between the triplet position of ligands and the emissive energy level of Ln^{3+} ions. The obtained $cbmp^-$ complexes display high quantum yields and long lifetimes compared with their corresponding ox^- complexes. The hydrated and D_2O-rehydrated phase of **3** and **4** were investigated to understand how the guest-molecules influence the luminescence behaviors. During the processes, the D_2O-induced structural phase transformations was observed, and the crystallinity produced more substantial change in the luminescence behaviors than removal and replacement of effective nonradiative relaxers. This research will provide insight into the correlation between structures and luminescence behaviors and help to synthesize materials incorporating the exquisite control of luminescence properties.

ASSOCIATED CONTENT

Supporting Information. Powder diffraction patterns, TGA curves, emission decay curves for complexes **1**−**4**. This material is available free of charge via the Internet at http://pubs.acs.org.

AUTHOR INFORMATION

Corresponding Author

*E-mail: rcao@fjirsm.ac.cn (R.C.), whsun@iccas.ac.cn (W.-H.S.).

ACKNOWLEDGMENT

This work was financially supported by the 973 Program (2011CB932504, 2007CB815303), NSFC (20731005, 20821061, and 91022007), NSF of Fujian Province (2006F3134), and Key Projects from CAS.

REFERENCES

(1) (a) Blasse, G.; Grabmaier, B. C. *Luminescent Materials*; Springer-Verlag: Berlin, Germany, 1994. (b) Bunzli, J.-C. G.; Piguet, C. *Chem. Soc. Rev.* **2005**, *34*, 1048. (c) Du, Y.-P.; Zhang, Y.-W.; Yan, Z.-G.; Sun, L.-D.; Yan, C.-H. *J. Am. Chem. Soc.* **2009**, *131*, 16364.

(2) Allendorf, M. D.; Bauer, C. A.; Bhakta, R. K.; Houk, R. J. T. *Chem. Soc. Rev.* **2009**, *38*, 1330.

(3) (a) Zhang, J.; Badger, P. D.; Geib, S. J.; Petoud, S. *Angew. Chem., Int. Ed.* **2005**, *44*, 2508. (b) Ronson, T. K.; Lazarides, T.; Adams, H.; Pope, S. J. A.; Sykes, D.; Faulkner, S.; Coles, S. J.; Hursthouse, M. B.; Clegg, W.; Harrington, R. W.; Ward, M. D. *Chem.—Eur. J.* **2006**, *12*, 9299.

(4) (a) White, K. A.; Chengelis, D. A.; Zeller, M.; Geib, S. J.; Szakos, J.; Petoud, S.; Rosi, N. L. *Chem. Commun.* **2009**, 4506. (b) Yan, X.; Cai, Z.; Yi, C.; Liu, W.; Tan, M.; Tang, Y. *Inorg. Chem.* **2011**, *50* (6), 2346.

(5) (a) Leininger, S.; Olenyuk, B.; Stang, P. J. *Chem. Rev.* **2000**, *100*, 853. (b) Tranchemontagne, D. J.; Ni, Z.; O'Keeffe, M.; Yaghi, O. M. *Angew. Chem., Int. Ed.* **2008**, *47*, 5136. (c) Seidel, S. R.; Stang, P. J. *Acc. Chem. Res.* **2002**, *35*, 972.

(6) (a) Zhu, X.; He, C.; Dong, D.; Liu, Y.; Duan, C. *Dalton Trans.* **2010**, *39*, 10051. (b) Reineke, T. M.; Eddaoudi, M.; Fehr, M.; Kelley, D.; Yaghi, O. M. *J. Am. Chem. Soc.* **1999**, *121*, 1651. (c) Pham, B. T. N.; Lund, L. M.; Song, D. *Inorg. Chem.* **2008**, *47*, 6329.

(7) de Lill, D. T.; de Bettencourt-Dias, A.; Cahill, C. L. *Inorg. Chem.* **2007**, *46*, 3960.

(8) (a) Herrera, J.-M.; Pope, S. J. A.; Adams, H.; Faulkner, S.; Ward, M. D. *Inorg. Chem.* **2006**, *45*, 3895. (b) Shavaleev, N. M.; Accorsi, G.; Virgill, D.; Bell, Z. R.; Lazarides, T.; Calogero, G.; Armaroli, N.; Ward, M. D. *Inorg. Chem.* **2005**, *44*, 61.

(9) (a) Cornil, J.; dos Santos, D. A.; Crispin, X.; Silbey, R.; Brédas, J. L. *J. Am. Chem. Soc.* **1998**, *120*, 1289. (b) Sato, S.; Wada, M. *Bull. Chem. Soc. Jpn.* **1970**, *43*, 1955.

(10) Latva, M.; Takalo, H.; Mukkala, V.-M.; Matachescu, C.; Rodriguez-Ubis, J. C.; Kankare, J. *J. Lumin.* **1997**, *75*, 149.

(11) (a) Song, X.; Zhou, X.; Liu, W.; Dou, W.; Ma, J.; Tang, X.; Zheng, J. *Inorg. Chem.* **2008**, *47*, 11501. (b) Daiguebonne, C.; Kerbellec, N.; Guillou, O.; Bünzli, J.-C.; Gumy, F.; Catala, L.; Mallah, T.; Audebrand, N.; Gérault, Y.; Bernot, K.; Calvez, G. *Inorg. Chem.* **2008**, *47*, 3700. (c) Marchal, C.; Filinchuk, Y.; Chen, X.-Y.; Imbert, D.; Mazzanti, M. *Chem.—Eur. J.* **2009**, *15*, 5273. (d) de Lill, D. T.; Gunning, N. S.; Cahill, C. L. *Inorg. Chem.* **2005**, *44*, 258. (e) Pellé, F.; Surblé, S.; Serre, C.; Millange, F.; Férey, G. *J. Lumin.* **2007**, *122*, 492.

(12) Sun, W.-H.; Hao, P.; Zhang, S.; Shi, Q.; Zuo, W.; Tang, X.; Lu, X. *Organometallics* **2007**, *26*, 2720.

(13) *CrystalClear*, Version 1.36; Rigaku Corporation: The Woodlands, TX, 2000.

(14) Sheldrick, G. M. *SHELXS-97, Program for Crystal Structure Solution and Refinement*; University of Göttingen: Göttingen, Germany, 1997.

(15) Ollendorff, W.; Weigel, F. *Inorg. Nucl. Chem. Lett.* **1969**, *5*, 263.

(16) (a) Brown, I. D.; Altermatt, D. *Acta Crystallogr.* **1985**, *B41*, 244. (b) Brese, N. E.; O'Keeffe, M. *Acta Crystallogr.* **1991**, *B47*, 19.

(17) (a) Sun, D. F.; Ma, S.; Ke, Y.; Petersen, T. M.; Zhou, H.-C. *Chem. Commun.* **2005**, 2663. (b) Duan, C.; Wei, M.; Guo, D.; He, C.; Meng, Q. *J. Am. Chem. Soc.* **2010**, *132*, 3321.

(18) Dexter, D. L. *J. Chem. Phys.* **1953**, *21*, 836.

(19) (a) Archer, R. D.; Chen, H. *Inorg. Chem.* **1998**, *37*, 2089. (b) Chen, W.; Fukuzumi, S. *Inorg. Chem.* **2009**, *48*, 3800.

(20) Soares-Santos, P. C. R.; Cunha-Silva, L.; Paz, F. A. A.; Ferreira, R. A. S.; Rocha, J.; Carlos, L. D.; Nogueira, H. I. S. *Inorg. Chem.* **2010**, *49*, 3428.

(21) (a) Eliseeva, S. V.; Bünzli, J.-C. G. *Chem. Soc. Rev.* **2010**, *39*, 189. (b) Song, Y.-S.; Yan, B.; Chen, Z.-X. *J. Solid State Chem.* **2004**, *177*, 3805.

(22) (a) Chen, X. Y.; Zhao, W.; Cook, R. E.; Liu, G. K. *Phys. Rev. B.* **2004**, *70*, 205122. (b) Chen, X .Y.; Liu, G. K. *J. Solid State Chem.* **2005**, *178*, 419.

(23) (a) Richardson, F. S.; Brittain, H. G. *J. Am. Chem. Soc.* **1981**, *103*, 18. (b) Bünzli, J.-C. G.; Choppin, G. R. *Lanthanide Probes in Life, Chemical and Earth Sciences. Theory and Practice*; Elsevier Science: New York, 1989.

(24) (a) Huang, Y.; Song, Y.-S.; Yan, B.; Shao, M. *J. Solid State Chem.* **2008**, *181*, 1731. (b) Bauer, C. A.; Timofeeva, T. V.; Settersten, T. B.; Patterson, B. D.; Liu, V. H.; Simmons, B. A.; Allendorf, M. D. *J. Am. Chem. Soc.* **2007**, *129*, 7136.

(25) (a) Stein, G.; Wurzburg, E. *J. Chem. Phys.* **1975**, *62*, 208. (b) Dew, W.; Jr, H.; Sudnick, D. R. *J. Am. Chem. Soc.* **1979**, *101*, 334. (c) Richardson, F. S. *Chem. Rev.* **1982**, *82*, 541. (d) Feng, R.; Jiang, F.-L.; Wu, M.-Y.; Chen, L.; Yan, C.-F.; Hong, M.-C. *Cryst Growth Des.* **2010**, *10*, 2306.

(26) Zhu, W.-H.; Wang, Z.-M.; Gao, S. *Inorg. Chem.* **2007**, *46*, 1337.